Received January 1997
Revised March 1998
Accepted June 1998

Three-dimensional simulation of natural convection in cavities with side opening

I. Sezai and A.A. Mohamad
Mechanical Engineering Department, Eastern Mediterranean University, North Cyprus, Mersin, Turkey

Introduction

Natural convection in open cavities has importance in simulating solar thermal receiver system[1], electronic cooling[2], energy saving in household refrigerators[3] and in fire precaution measures[4]. For steady state conditions, several works were published in two-dimensional simulation of natural convection in open cavities[5-14]. Recently, attention was given for transient simulation of natural convection in open cavity[15,16]. The major conclusions of the mentioned works are that the flow becomes unstable for Ra = 1×10^7 and average Nusselt number is not a strong function of the inclination angle. For large Ra the rate of heat transfer along the heated wall approaches those of a flat plate. For Ra $\geq 1 \times 10^5$, a recirculation was predicted at the top corner of the cavity. Also, it was found that the flow is thermally stratified at the top wall. As far as three-dimensional simulation is considered, we have not encountered cited work in open literature. Three-dimensional simulation is more realistic than two-dimensional approximation and it may be used to test the validity of two-dimensional results. Accordingly, fluid flow and heat transfer in open cavity is studied in this work. Flow is induced in the cavity due to heating of the far end vertical wall, where other walls are thermally insulated (see Figure 1). The opposing vertical face to the heated vertical wall is open to a large reservoir (ambient) at a temperature lower than the heated wall. Hence, natural convection is initiated by induced flow adjacent to the hot wall. It is expected that the flow enters the cavity from the lower portion of the opening and leaves from upper portion of the opening. Two- and three-dimensional simulations are performed for the mentioned geometry for Rayleigh numbers of 10^3 to 10^6 where Prandtl number is kept constant at 0.71 (air). Aspect ratio in lateral direction A_y (= B/H) is changed in the range of 0.125 to 2.0, to validate the two-dimensional predictions.

It is found that the rate of heat transfer predicted by two-dimensional model is well compared with 3-D model for Ra < 10^5. For Ra > 10^5 lateral side walls effects increase, necessitating the use of a three-dimensional model.

International Journal of Numerical Methods for Heat & Fluid Flow
Vol. 8 No. 7, 1998, pp. 800–813.

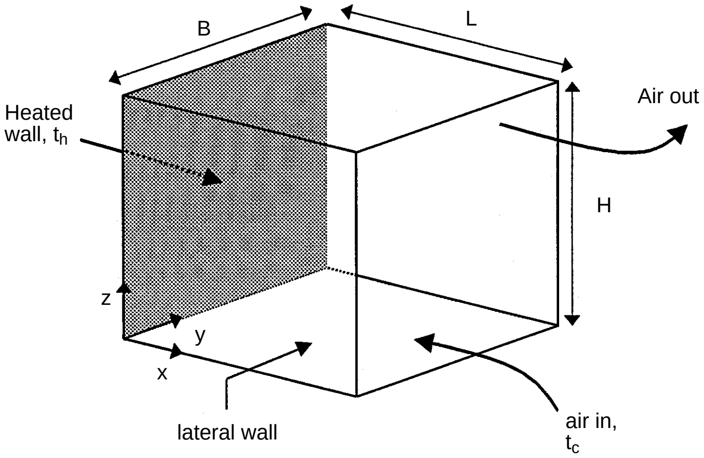

Figure 1.
Schematic diagram and coordinate system of open end cavity

Analysis

Governing equations

Figure 1 shows the schematic diagram of the problem with the Cartesian coordinate system. In nondimensional form the conservation equations, governing the transport of mass, momentum and energy with Boussinesq approximation, can be written as

continuity,

$$\frac{\partial U}{\partial X}+\frac{\partial V}{\partial Y}+\frac{\partial W}{\partial Z}=0 \tag{1}$$

x-momentum,

$$\frac{\partial U}{\partial X}+V\frac{\partial U}{\partial Y}+W\frac{\partial U}{\partial Z}=-\frac{\partial P}{\partial X}+\nabla^2 U \tag{2}$$

y-momentum,

$$\frac{\partial V}{\partial X}+V\frac{\partial V}{\partial Y}+W\frac{\partial V}{\partial Z}=-\frac{\partial P}{\partial Y}+\nabla^2 V \tag{3}$$

z-momentum,

$$\frac{\partial W}{\partial X}+V\frac{\partial W}{\partial Y}+W\frac{\partial W}{\partial Z}=-\frac{\partial P}{\partial Z}+\nabla^2 W+RaT \tag{4}$$

energy

$$\frac{\partial T}{\partial X}+V\frac{\partial T}{\partial Y}+W\frac{\partial T}{\partial Z}=\frac{1}{\mathbf{Pr}}\nabla^2 T \tag{5}$$

Boundary conditions are as follows

$$U = V = W = 0, \quad X = 0 \tag{6a}$$

$$\frac{\partial U}{\partial X} = \frac{\partial V}{\partial X} = \frac{\partial W}{\partial X} = 0, \quad X = L/H \tag{6b}$$

$$U = V = W = 0, \quad Y = 0, B/H \tag{7}$$

$$U = V = W = 0, \quad Z = 0, 1 \tag{8}$$

where the above equations are nondimensionalized by defining $X = x/H$, $Y = y/H$, $Z = z/H$, $P = p/\rho U_r^2$, $U_r = \nu/H$, $U = u/U_r$, $V = v/U_r$, $W = w/U_r$, $T = (t-t_c)/(t_h-t_c)$. As shown in Figure 1, B, H and L stand for width, height and length of the cavity, respectively. P and T are nondimensional pressure and temperature. U, V and W are the nondimensional velocity components in x, y and z-directions respectively. The other nondimensional parameters in the above equations are Prandtl number Pr = ν/α, Rayleigh number Ra = $g\beta\Delta t H^3/\nu\alpha$ where β, ν, and α are the coefficient of volumetric expansion, kinematics viscosity, and thermal diffusivity. Δt is the temperature difference (t_h-t_c), where t_h is the temperature of the heated wall and t_c is the temperature of the ambient.

The left vertical wall is heated while all other walls are insulated. The boundary conditions for the temperature are

$$\frac{\partial T}{\partial Y} = 0, \quad Y = 0, B/H \tag{9}$$

$$\frac{\partial T}{\partial Z} = 0, \quad Z = 0, 1 \tag{10}$$

$$T = 1, \quad X = 0 \tag{11}$$

$$T=0 \text{ at } X = L/H \quad \text{if } U < 0 \tag{12a}$$

$$\frac{\partial T}{\partial X} = 0 \text{ at } \mathrm{X = L/H} \quad \text{if } \mathrm{U} > 0 \tag{12b}$$

Nusselt number is defined as,

$$Nu = \frac{hH}{k} \tag{13a}$$

where h and k are heat transfer coefficient and thermal conductivity respectively. Nusselt number can be deduced from temperature field by the following formula:

$$Nu = \frac{\partial T}{\partial X} \tag{13b}$$

Laterally averaged quantities are defined as $\int_0^{B/H} \phi dY$, where ϕ stands for the variable to be averaged, such as Nu, U, etc.

Method of solution

Equations (1)-(5) are discretized using the staggered, nonuniform control volumes. In order to minimize the numerical diffusion errors, a third order accurate QUICK scheme[17] is used in approximating the advection terms. However, QUICK scheme suffers from a lack of boundedness, i.e. it tends to give rise to non-physical oscillations in high gradient regions (numerical dispersion). Flux limiter is a remedy for such problems. Hence, a limiter, known as ULTRA-SHARP[18,19] is used. This high order scheme proved to be superior to low order schemes. SIMPLE algorithm is used to couple momentum and continuity equations. The resulting set of linearized algebraic equations are solved iteratively by Bi-CGSTAB method[20] using SSOR preconditioning.

Grid independent solutions are ensured by comparing the results of different grid meshes for Ra $= 1 \times 10^6$, which is the highest Rayleigh number investigated. Figure 2 shows the test results for laterally averaged values of Nu on the heated wall and U-velocity at the opening, on vertical mid-plane for the cubic cavity. The difference between predictions of $50 \times 50 \times 50$ and $60 \times 60 \times 60$ grid sizes is insignificant. Hence, all calculations are performed with $50 \times 50 \times 50$ grids.

Results and discussions

Results are presented for natural convection in open cavities for 2 and 3-D simulations for Ra in the range 10^3-10^6. To investigate the effect of three-dimensionality, calculations were made for lateral aspect ratios (A_y) of 2.0, 1.0, 0.5, 0.25 and 0.125 and for L/H of unity. The predictions of 2-D and 3-D cubic cavity are also compared and discussed.

In Figures 3 and 4, the 2-D and 3-D results are compared for laterally averaged U-velocity (averaged in y-direction) at the opening of the cavity and laterally averaged Nusselt number on the hot wall respectively. As Rayleigh number increases the difference between the results of 2-D and 3-D simulations becomes significant, specially for U-velocity. It should be noted that these results are for cubic cavity where B/H and L/H are unity. The difference between predictions of the two models for Nu is not that significant for Ra $< 1 \times 10^5$. For Ra $\geq 1 \times 10^5$, 2-D simulation under-predicts the rate of heat transfer, compared with 3-D model. The average Nusselt number, $\int NudYdZ$, predicted by 3-D and 2-D models are summarized in Table I. For Ra$=1 \times 10^3$, the heat transfer

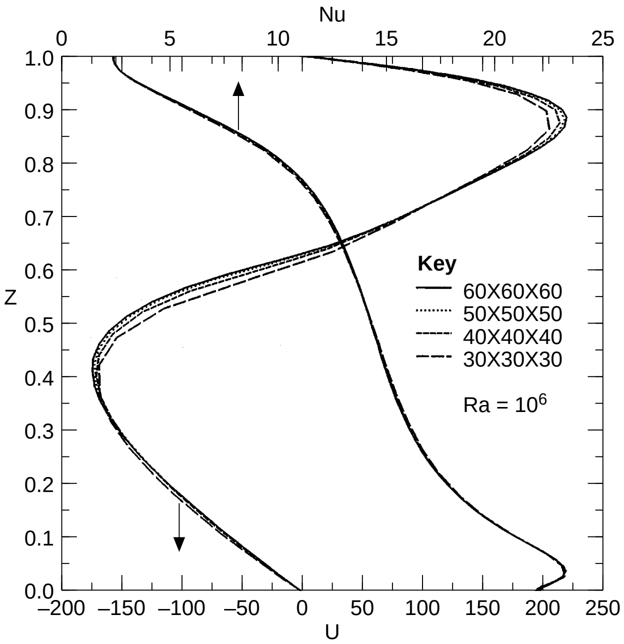

Figure 2.
Grid independence test: laterally averaged Nusselt number and laterally averaged *U*-velocity at the central vertical plane at open end for Ra = 1×10^6

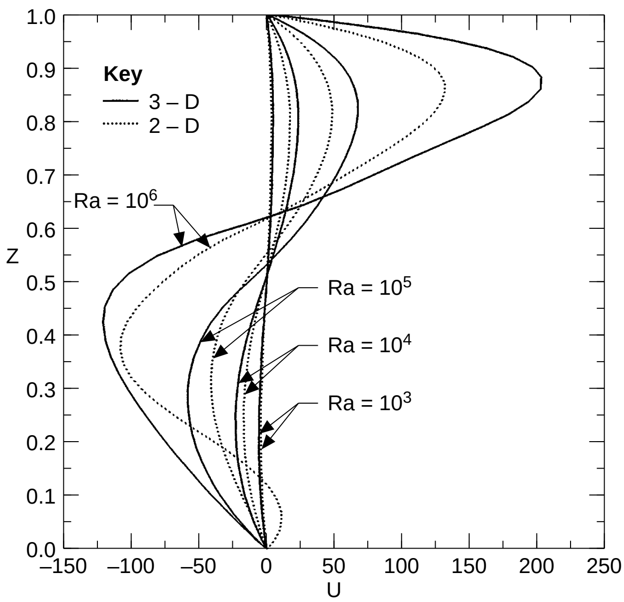

Figure 3.
Comparison of laterally averaged U-velocity profile of 3-D simulation with 2-D results at open end of cavity

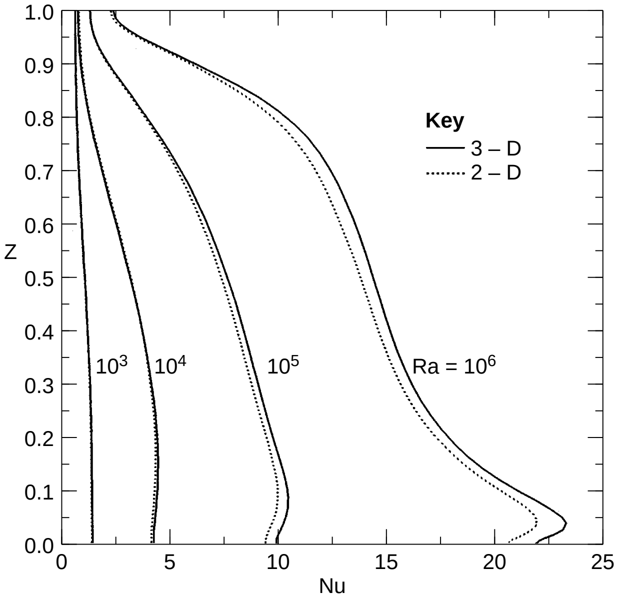

Figure 4. Comparison of the laterally averaged Nusselt number predicted by 3-D simulation with that of 2-D results

is conduction dominated, i.e., Nu ≅ 1.0. The difference between the predictions of 2-D and 3-D is in the second significant digits for Ra$<1\times10^5$. For Ra $> 1\times10^5$ the difference between 2-D and 3-D predictions becomes greater than 4 per cent.

In order to illustrate the three-dimensionality of the flow, U-velocity profiles are plotted in Figure 5 at the opening of the cavity for Rayleigh numbers of 1×10^4, 1×10^5 and 1×10^6 where it is observed that the flow is three-dimensional. For Ra$=1\times10^6$, the three-dimensionality of the flow is more profound. Figure 6 shows the vertical velocity component (W) at mid-horizontal plane for Rayleigh numbers of 1×10^4, 1×10^5 and 1×10^6 for a cubic cavity. The three-dimensionality of the flow at the lateral ends is clearly evident. W velocity profile at mid section of the cavity (Y = 0.5, Z = 0.5) is quantitatively displayed in Figure 7 where it can be observed that the magnitude of the velocity increases while the boundary layer thickness decreases as Ra increases.

The variation of the vertically averaged Nusselt number ($\int_0^1 NudZ$) is shown in Figure 8 for different Rayleigh number for a cubic cavity. It is evident that the Nusselt number does not vary appreciably in Y-direction except near lateral

Ra	Nu 2-D	Nu 3-D
10^3	1.033	1.040
10^4	2.851	2.864
10^5	6.630	6.872
10^6	13.358	13.961

Table I. Average Nusselt number predicted by 2-D and 3-D for cubic cavity

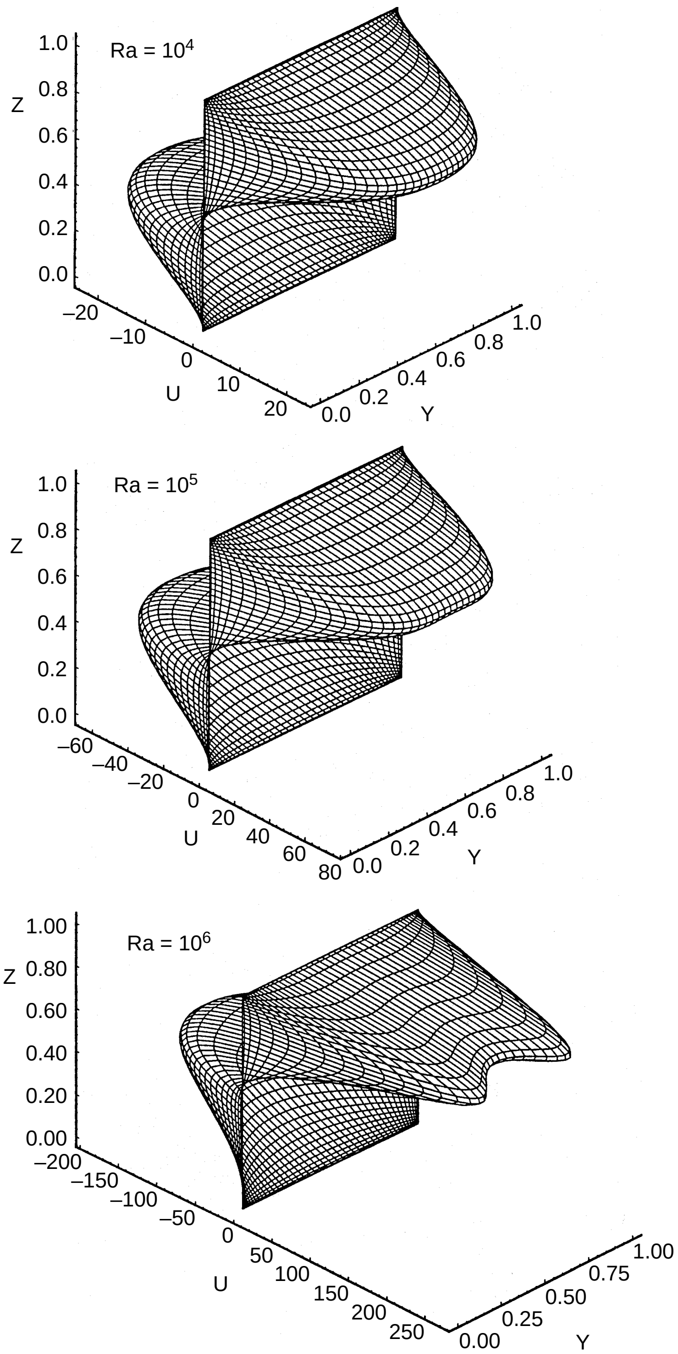

Figure 5.
U-velocity profiles at the open end of the 3-D open cavity for Ra = 1×10^4, 1×10^5 and 1×10^6

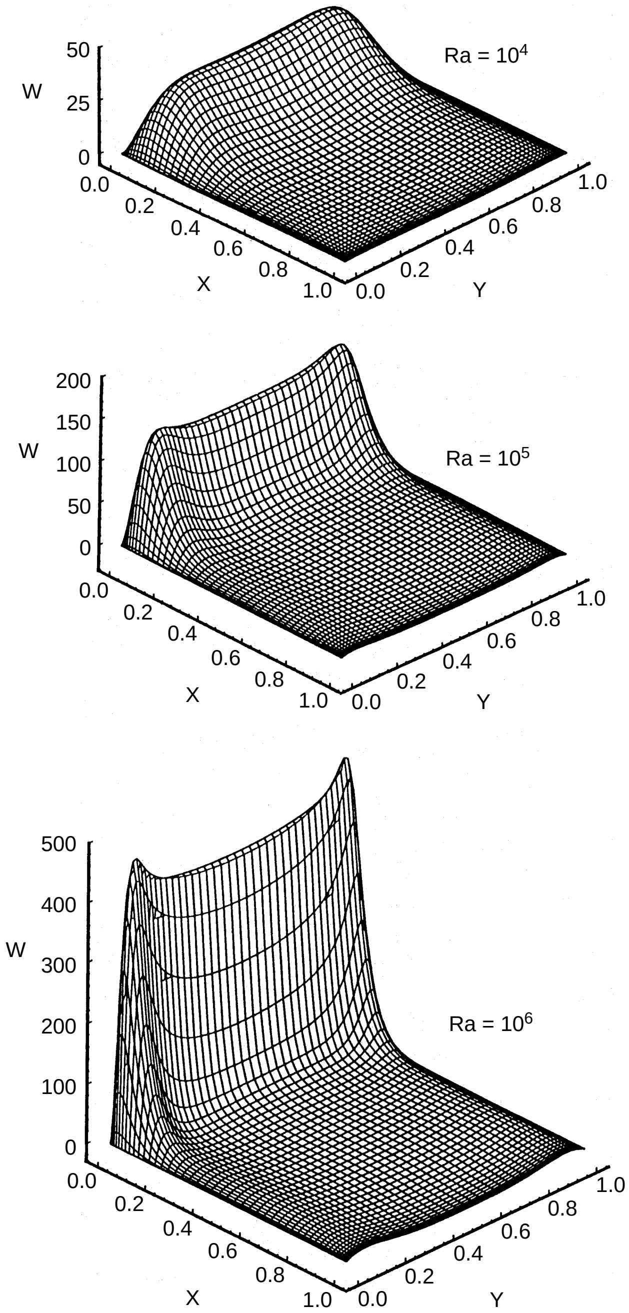

Figure 6.
W-velocity profiles at the central horizontal plane section of the cavity for Ra = 1×10^4, 1×10^5 and 1×10^6

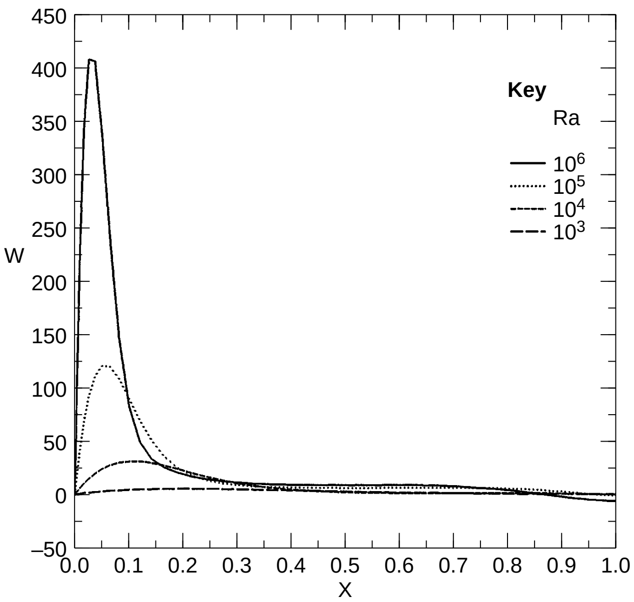

Figure 7.
W-velocity profiles at Z = 0.5, Y = 0.5 for different Rayleigh numbers

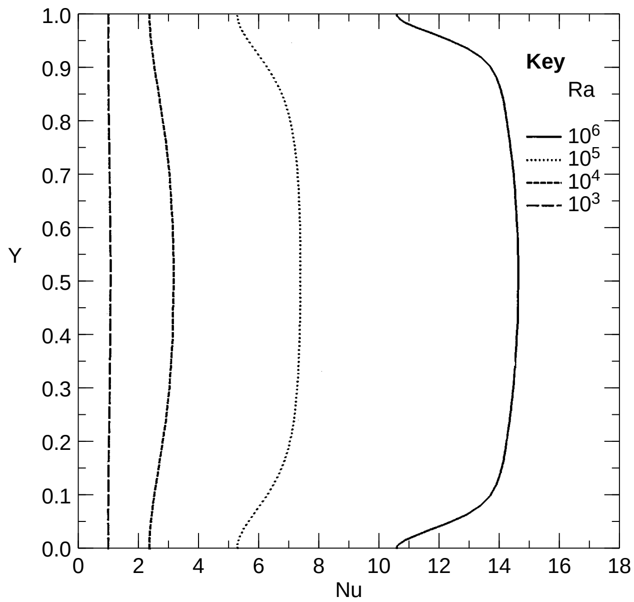

Figure 8.
Variation of vertically averaged Nusselt number along lateral direction

surfaces where it decreases. This decrease in Nusselt number is more pronounced at high Rayleigh numbers. On the other hand laterally averaged Nusselt number on the heated wall decreases in the vertical direction as shown in Figure 2. This is due to the fact that the thermal boundary layer is thinner at the bottom and becomes thicker at the top of the heated wall.

Effect of aspect ratio A_y on the variation of laterally averaged Nusselt number is illustrated in Figure 9 as a function of Z. The average Nusselt number is maximum for $A_y = 2$ (wider cavity) and decreases as the aspect ratio decreases (narrower cavities). The difference in Nu for aspect ratios of 2.0 and 1.0 are not significant but this difference becomes considerable for very narrow cavity ($A_y = 0.125$). The average Nusselt number predicted for A_y of 2.0, 1.0, 0.5, 0.25 and 0.125 are 14.11, 13.96, 13.67, 12.77 and 10.75 respectively. It can be concluded that for cavities of A_y greater than unity, the Nusselt number is not a strong function of the lateral aspect ratio. The variation of vertically averaged Nusselt number is shown in Figure 10 as a function of Y for different lateral aspect ratios. It can be noticed that the peak value of Nusselt number is almost constant (14.2-14.8) for aspect ratios of 2.0, 1.0 and 0.5. For the narrow cavity ($A_y = 0.125$) the Nusselt number drastically decreases due to hydraulic resistance, where flow into cavity is severely restricted. Also, it can be noticed that the peak value of Nu is at the center of the cavity.

Stream lines at the mid plane of the cavity are shown in Figure 11 a, b, c and d for lateral aspect ratios, A_y, of 2.0, 0.5, 0.25 and 0.125 respectively, for $Ra=10^6$. It is interesting that the recirculation eye moves toward center as the lateral aspect ratio decreases and totally diminishes for narrow cavities ($A_y<0.5$). Also, the area occupied by the exit flow at the opening increases for narrower cavities. For $A_y=0.125$ the outflow occupies about 50 per cent of the opening whereas it occupies only 35 per cent for $A_y=2.0$.

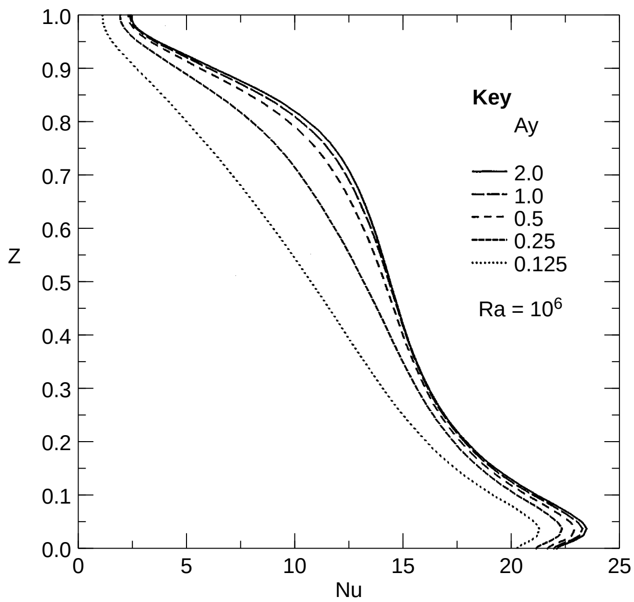

Figure 9.
Variation of laterally averaged Nusselt number along vertical direction for different aspect ratios

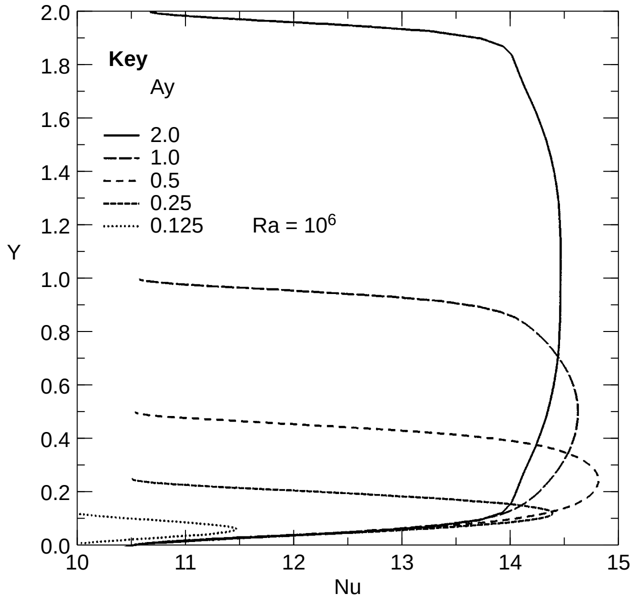

Figure 10.
Variation of vertically averaged Nusselt number along y-direction for different lateral aspect ratios

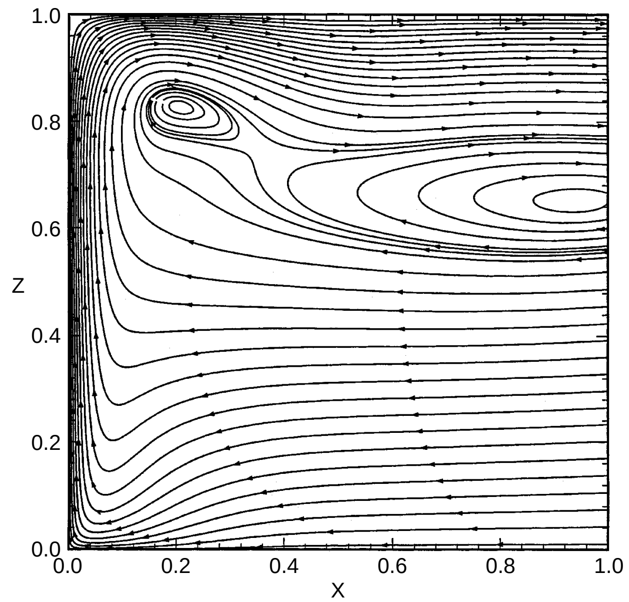

Figure 11a.
Stream lines at mid vertical plane for Ra = 10^6 for cavities with A_y = 2.0

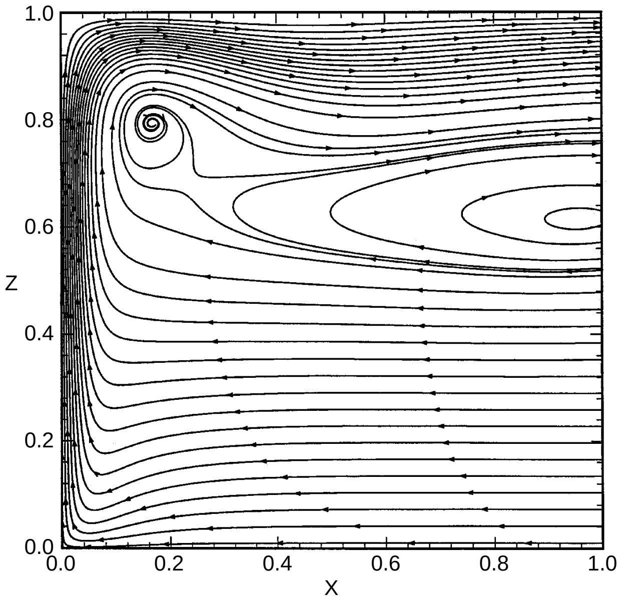

Figure 11b.
Stream lines at mid-vertical plane for $Ra = 10^6$ for cavities with $A_y = 0.5$

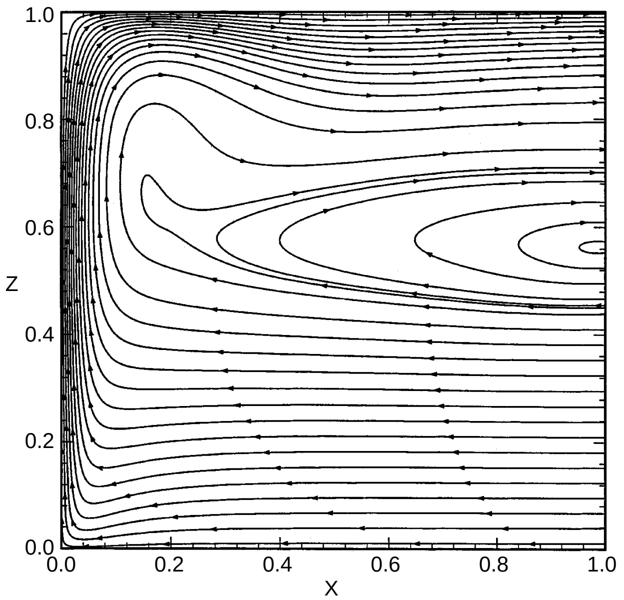

Figure 11c.
Stream lines at mid-vertical plane for $Ra = 10^6$ for cavities with $A_y = 0.25$

Conclusions

The three-dimensional effects in the open cavity problem heated from the opposite vertical wall are investigated and the results are compared with 2-D simulations. The results show that there is a difference in the Nusselt number predicted by the two models for Rayleigh numbers 10^5 and above. The flow

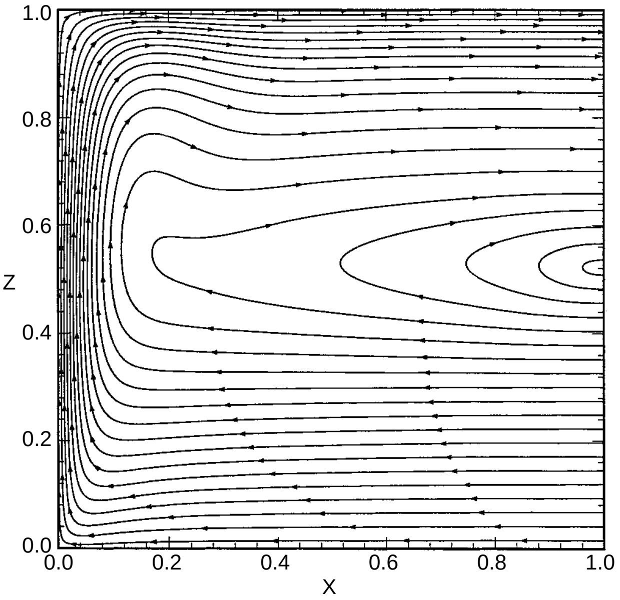

Figure 11d. Stream lines at mid-vertical plane for Ra = 10^6 for cavities with A_y = 0.125

structure attains a three-dimensional nature at Ra = 10^6, where changes in U and W velocities along lateral direction become noticeable. The resulting change in the Nusselt number along the lateral direction is demonstrated with calculations made at different lateral aspect ratios at this Rayleigh number. The effect of the lateral walls on the Nusselt number is more emphasized for a lateral aspect ratio of 0.125 which represents a very narrow cavity. The results indicate that three-dimensional simulations are necessary for open cavities at Rayleigh numbers above 1×10^5. The effect of lateral walls increases as lateral aspect ratio (A_y) decreases.

It can be concluded that two-dimensional results are valid for lateral aspect ratio equal and greater than unity and for Rayleigh number equal and less than 1×10^5.

References

1. Clausing, A.M., "Convective losses from cavity solar receivers – comparisons between analytical predictions and experimental results", *J. Solar Eng.,* Vol. 105, 1993, pp. 29-33.
2. Behnia, M. and De Vahl Davis, G., "Natural convection cooling of an electronic component in a slot", *Proc. of the Ninth Int. Heat Transfer Conf.*, Vol. 2, 1990, pp. 343-8.
3. Skok, H., "Buoyancy driven flow and heat transfer in a side facing open cavity with application to heat transfer in a household refrigerator", MSME thesis, Purdue University, 1988.
4. Jones, G.F. and Cai, J., "Analysis of a transient asymmetrically heated/cooled open thermosyphon", *J. Heat Transfer*, Vol. 115, 1993, pp. 621-30.
5. Lighthill, M.J., "Theoretical considerations on free convection in tubes", *Quart. J. Mech. Appl. Math.*, Vol. 6 No. 398, 1953.

6. Martin, B.W., and Cohen H., "Heat Transfer by free convection in an open thermosyphon tube", *Br. J. Appl. Phys.*, Vol. 5, 1954, pp. 91-5.
7. Gosman, A.D., Lockwood, F.C. and Tatchell, D.G., "A numerical study of the heat transfer performance of the open thermosyphon", *Int. J. Heat Transfer,* Vol. 14, 1971, pp. 1717-30.
8. Bejan, A. and Kimura, S., "Penetration of free convection into a lateral cavity", *J. Fluid Mech*, Vol. 103, 1981, pp. 465-78.
9. Chan, Y.L. and Tien, C.L., "A numerical study of two-dimensional laminar natural convection in shallow open cavities", *Int. J. Heat Mass Transfer,* Vol. 28, 1985, pp. 603-12.
10. Skok, H., Ramadhyani, S. and Schoenhals, R.J., "Natural convection in a side facing open cavity", *Int. J. Heat and Fluid Flow*, Vol. 12, 1991, pp. 36-45.
11. Lage, L.J., Lim, J.S. and Bejan, A., "Natural convection with radiation in a cavity with open top end", *J. Heat Transfer,* Vol. 114, 1992, pp. 479-86.
12. Showole R.A. and Tarasuk, J.D., "Experimental and numerical studies of natural convection with flow separation in upward facing inclined cavities", *J. Heat Transfer*, Vol 115, 1993, pp. 592-605.
13. Mohamad, A.A., "Natural convection in open cavities and slots", *J. Num. Heat Transfer,* part A, Vol. 27, 1995, pp. 705-16.
14. Hess, F.C. and Henze, R.H., "Experimental investigation of natural convection losses from open cavities", *J. Heat Transfer,* Vol. 106, 1984, pp. 333-8.
15. Merrikh, A.A. and Mohamad, A.A., "Transient natural convection in side opening cavities", *Proc. of the First Int. Transient Convective Heat Transfer Conf.,* 1996.
16. Merrikh, A.A., "Transient natural convection in open cavities", MSME Thesis, Eastern Mediterranean University, 1996.
17. Leonard, B.P., "A stable and accurate convective modelling procedure based on quadratic upstream interpolation", *Comput. Methods Appl. Mech. Engng.*, Vol. 19, 1979, pp. 59-98.
18. Leonard, B.P. and Mokhtari, S., "Beyond first order upwinding: the ULTRA-SHARP alternative for nonoscillatory steady-state simulation of convection", *Int. J. Numer. Methods Eng.*, Vol. 30, 1990, pp. 729-66.
19. Leonard, B.P. and Drummond, J.E., "Why you should not use 'hybrid', 'power law' or related exponential schemes for convective modelling – there are much better alternatives", *Int. J. Numer. Meth. Fluids,* Vol. 20, 1995, pp. 421-42.
20. Van der Vorst, H.A., "BiCGSTAB: a fast and smoothly converging variant of Bi-CG for the solution of non-symmetric linear systems", *SIAM J. Sci. Statist. Comput.*, Vol. 13, 1992, pp. 631-44.